Geoderma 447 (2024) 116924

Contents lists available at ScienceDirect

Geoderma

journal homepage: www.elsevier.com/locate/geoderma

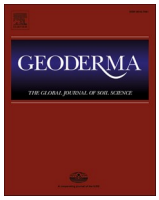

Microbial decomposition of organic matter and wetting–drying promotes aggregation in artificial soil but porosity increases only in wet-dry condition

Sheikh M.F. Rabbi [a,b,*], Charles R. Warren [a], Brad Swarbrick [c], Budiman Minasny [a], Alex B. McBratney [a], Iain M. Young [a,d]

[a] School of Life and Environmental Sciences, Faculty of Science, The University of Sydney, Camperdown, NSW 2006, Australia
[b] Department of Agriculture and Fisheries, Queensland Government, Toowoomba, QLD 4350, Australia
[c] School of Chemistry, Faculty of Science, The University of Sydney, Camperdown, NSW 2006, Australia
[d] Division of Biological and Environmental Science and Engineering, King Abdullah University of Science and Technology, Thuwal 23955, Saudi Arabia

ARTICLE INFO

Handling Editor: N. Nunan

Keywords:
Soil respiration
Microbially derived carbon
Phospholipid fatty acid
Porosity
Metabolites
Tomography

ABSTRACT

Aggregation is one of the key properties influencing the function of soils, including the soil's potential to stabilise organic carbon and create habitats for micro-organisms. The mechanisms by which organic matter influences aggregation and alters the pore geometry remain largely unknown. We hypothesised that rapid microbial processing of organic matter and wetting and drying of soil promotes aggregation and changes in pore geometry. Using microcosms of silicate clays and sand with either rapidly decomposable glucose or slowly decomposable cellulose, the degree of aggregation ($P < 0.001$), was greater in glucose treatments than controls that did not receive added carbon or microbial inoculum. We link this to microbial activity through measurements in soil respiration, phospholipids and microbially derived carbon. Our results demonstrate that rapid microbial decomposition of organic matter and microbially derived carbon promote aggregation and the aggregation process was particularly strong in the wet-dry condition (alternating between 30 % and 15 % water content) with significant modification of porosity ($P < 0.05$) of the aggregates.

1. Introduction

Aggregation is one of the most important soil processes that creates and modifies the physical architecture of soil (Tisdall and Oades, 1982). Clay minerals and microbial polysaccharides function as cementing agents, while plants roots and fungal hyphal networks bind the soil together into structures (Southard and Buol, 1988; Oades, 1993; Lavelle et al., 2020). Organic matter acts as a substrate and supports microbial activity and growth. Adsorption of microbial metabolites and organic matter decomposition products on mineral surfaces are likely to be involved in aggregate formation (Golchin et al., 1994; Rabbi et al., 2020). Under field conditions the effect of organic matter on aggregate stability or aggregate-size distribution may be masked by multiple factors, such as climatic conditions, soil texture, clay minerals, soil water dynamics and antecedent organic matter content (Abiven et al., 2009). Nevertheless, experiments under controlled conditions have begun to uncover the myriad of interacting factors contributing to aggregation.

One of the most important abiotic processes responsible for aggregation are wetting–drying cycles that create and modify pore structures depending on the nature of the clay minerals (Turk et al., 2011; Diel et al., 2019; Xu et al., 2021). The stress generated by the wetting–drying at different water potentials (up to −100 kPa) increases aggregation, while the same force can destabilise the aggregates during rapid wetting and drying cycles (Utomo and Dexter, 1982; Xu et al., 2021). Moreover, wetting and drying may influence the microbial processing of organic matter by altering the accessibility of microbes to decomposition sites (Nunan et al., 2017), thereby limiting the contribution of microbial processing to aggregation.

Here, we sought to understand whether the microbial processing of added organic matter can initiate aggregation with concomitant modification of pore geometry under wet and wet-dry water regimes. Considering the complexity of microbially mediated aggregation of soil particles, we deployed a range of physical, microbiological, biochemical and spectroscopic imaging approaches to decipher the role of microbial

* Corresponding author at: School of Life and Environmental Sciences, Faculty of Science, The University of Sydney, Camperdown, NSW 2006, Australia.
E-mail address: sheikh.rabbi@sydney.edu.au (S.M.F. Rabbi).

https://doi.org/10.1016/j.geoderma.2024.116924
Received 10 May 2023; Received in revised form 10 March 2024; Accepted 17 May 2024
Available online 22 May 2024

processing of organic matter in soil aggregation and pore architecture changes. The experimental hypothesis was that rapid microbial decomposition of organic matter promotes aggregation with associated changes in pore geometry and alternating wetting–drying of soil also affects aggregation. To test the hypothesis, we compared the microbial processing of organic matter in glucose (rapid decomposition), or cellulose (slow decomposition) treated artificial model soils under wet and wet-dry water regimes. We used water-stable aggregate content as a metric for aggregation in soil, aggregate porosity and pore size distribution to represent the change in pore geometry in newly formed aggregates. To demonstrate microbial activity we determined soil respiration, microbial carbon, fungi:bacteria ratio, extracellular metabolite concentration. To assess abiotic drivers of aggregation, a subset of microcosms was microbially suppressed and did not receive any organic matter.

2. Materials and methods

2.1. Experimental setup and measurements

2.1.1. Soil microcosm

We examined the effects of carbon substrates (glucose and cellulose) and water treatments (wet and wet-dry) on aggregation via a fully factorial experiment with 4 replicate microcosms (i.e. 2C treatments × 2 water treatments × 4 replicate mesocosms). The application rate of glucose and cellulose was 2.5 g C 100 g soil^{-1}, which was based on the soil carbon stock in a native pasture of south-eastern Australia, 33 Mg C ha^{-1} (Rabbi et al., 2015a). To assess abiotic drivers, we also maintained four replicates of a control without carbon and microbial inoculation. Soil microcosms were composed of reagent grade silica sand (60 %), montmorillonite (30 %) and kaolinite clays (10 %) (Sigma-Aldrich®). The maximum and minimum particle sizes of the sand were 250 and 125 μm, and the size of montmorillonite and kaolinite particles was < 50 μm. The reagent grade sand and clay minerals used were free of any organic matter and aggregation to allow a better understanding of the influence of each factor. Like natural soil, the artificial soil (henceforth termed soil) had texture and different types of clay minerals that we assumed to be sufficient to form aggregates in presence of organic matter and microbes. The soil materials in the microcosms (100 g) were mixed with either glucose or cellulose to achieve a carbon content of 2.5 g (100 g soil)$^{-1}$. The soils were inoculated with microbes extracted from the surface horizon of a Luvisol (WRB, 2015)) located at Lansdowne farm, University of Sydney, Camden, NSW. The microbial biomass carbon of the soil measured using the substrate induced respiration method (Anderson and Domsch, 1978) was 160 μg (g soil) $^{-1}$ (unpublished data). The microbes were extracted with ¼ Ringer's solution (soil: solution was 1:10 w/v) (Rabbi et al., 2020). Freshly prepared 1 ml of microbial extract was added to 8 ml 5 mM N nutrient solution (Dechorgnat et al., 2018), mixed thoroughly and added to the soil. The carbon added with microbial inoculum was negligible because it would have increased soil organic carbon by a maximum of 0.16 μg g^{-1} (assuming Ringer's solution extracted 100 % of microbial biomass carbon). To assess abiotic drivers of aggregation, 4 replicate microcosms that did not receive organic matter or microbial inoculum and thereby served as microbially suppressed controls to compare with inoculated treatments.

The microcosms were incubated at 25 °C on tension tables and maintained at −10 kPa (gravimetric water content of 30 % (w/w)). Half of the treatments were maintained under alternating wet-dry moisture conditions. The wet-dry water treatments were removed from the tension table every 14 days to allow the water content of the soils to dry to 15 % (w/w) (−50 kPa) before placed again on the tension table. The wet-dry treatments were weighed every second day to check the water content of the soils. The wet treatments were also weighed every two weeks and the water content measured. The microcosms were incubated for 180 days.

2.1.2. Soil respiration

Soil respiration of each sample was measured after 30, 60, 90 and 180 days of incubation using a closed gas exchange system comprising a non-dispersive infrared K30 CO_2 sensor, small fan, and a combined temperature, humidity, and barometric pressure sensor (Adafruit BME320). To calibrate the K30 sensors we used certified 400 and 2000 ppm CO_2 (BOC®, Australia) and applied a minor correction for the effect of humidity on CO_2 calibration. Respiration was determined in microcosms incubated in a closed Mason jar for 1 h at 25 °C, with measurements every 30 s. Respiration data for 180 days are shown here and additional data on soil respiration are presented in the Supplementary Materials. The soil respiration rate was calculated using the CO_2 concentration as described in Witzgall et al. (2021):

$$\frac{\mu gCO_2 - C}{h} = \frac{\Delta CO_2}{\Delta t} \times \frac{1}{10^6} \times \frac{V}{VIG} \times M \times 60 \times 1000 \quad (1)$$

where, $\frac{\Delta CO_2}{\Delta t}$ = change in CO_2 ppm over incubation time (min), V = headspace volume (mL), VIG = volume of ideal gas at 25 °C was 24.45 mL mol^{-1}, h = hour, M = atomic mass of carbon

2.1.3. Aggregate mass

Water stable aggregate mass (500 – 2000 μm) was determined using a bespoke Cornell Rainfall Simulator (Moebius-Clune et al., 2016), which supplied steady water flow from an overhead water tank on a sieve stack (2000 and 500 μm sieves) containing a known weight of soil. After measuring respiration, 30 g moist soil subsample was placed on the top sieve. The sieve stack was placed on a sieve holder attached to a reciprocating shaker. The soil sample was wet sieved for 4 min while shaking at 100 rpm under a continuous flow of water supplied through a circular head connected to an overhead 20 L water tank. The total kinetic energy supplied during wet sieving of each sample was 0.18 J. After sieving, the aggregates retained on the top 2000 and 500 μm sieves were transferred to plastic cups and dried at 40 °C for 48 h and used for calculating aggregate mass. Total aggregate mass represents the state of aggregation in the incubated soils.

2.1.4. Aggregate carbon and $\delta^{13}C$ enrichment

The carbon concentration and $\delta^{13}C$ enrichment in the aggregates were measured using a Thermo Delta V isotope ratio mass spectrometer (IRMS) coupled to ConfloIV and FlashHT peripherals (Thermo Fisher, Bremen, Germany). The values of control soil and the added glucose and cellulose were also measured. The values of $\delta^{13}C$ were expressed in parts per mil (‰) relative to the VPDB (Vee Pee Dee Belemnite) standard. The $\delta^{13}C$ values of pure glucose and cellulose were −11.04 ‰ and −26.31 ‰, respectively. The fraction of carbon in aggregates derived from the microbes (f) was calculated using the two-source isotopic mixing model (Pausch and Kuzyakov, 2012):

$$f = \frac{\left(\delta^{13}C_{aggregate} - \delta^{13}C_{glucose/cellulose}\right)}{\left(\delta^{13}C_{microbes} - \delta^{13}C_{glucose/cellulose}\right)} \quad (2)$$

$\delta^{13}C_{glucose/cellulose}$ was $\delta^{13}C$ of pure glucose or cellulose and $\delta^{13}C_{microbes}$ was the $\delta^{13}C$ of soil that had microbes but no glucose or cellulose (−28.79 ‰). To determine the microbial $\delta^{13}C_{microbes}$ an additional set of microcosms were maintained, which received microbial inoculation and nutrient solution but did not receive any carbon addition. Any microbial growth in this soil was used to determine the $\delta^{13}C_{microbes}$. For the control, the $\delta^{13}C$ value of $\delta^{13}C_{glucose/cellulose}$ were not included in the equation (2). The 95 % confidence interval of the isotopic estimation was calculated using '*IsoError*' (https://www.epa.gov/eco-research/stable-isotope-mixing-models-estimating-source-proportions) based on the measured standard deviation of $\delta^{13}C$ in aggregate, glucose, cellulose, and microbes (Phillips and Gregg, 2001).

To visualise and identify microbially derived carbon on the aggregates, we used a Raman imaging microscope (RA816 BioAnalyzer, Reinshaw, UK) to generate chemical maps of proteins, lipids,

phospholipids, and amides in prepared samples. Raman spectra (change in intensity (e.g. counts) of the incident light due to change in molecular polarizability (Bergholt et al., 2019)) were acquired in the range 400–1900 cm^{-1}. The surface of the aggregate was mapped by setting up a grid using StreamlineTM image acquisition software, where the area of each cell in the grid was equal to the microscope field of view. The entire grid was scanned to obtain Raman spectra. The acquired spectra was clustered into groups using principal component analysis (see Supplementary Materials). Each cluster was labelled with a false colour (either red, blue, green, or yellow). Loadings of each cluster were then used to reconstruct the spectra in WiRE software version 5.4. Reinshaw, UK. Raman spectra were corrected using cosmic ray removal and noise filtering prior to analysis. The Raman peaks were assigned to proteins, lipids, phospholipids, and amides (Movasaghi et al., 2007) to visualise the presence of microbially derived carbon on the aggregates. We used aggregates from glucose treatments with 2.5 % carbon and control under wet and wet-dry conditions for Raman microscopy since aggregation was observed to be greatest in the 2.5 % carbon containing glucose treatments. Moreover, to avoid the interference of undecomposed cellulose with microbially derived carbon in aggregates during Raman microscopy we excluded cellulose treatments from imaging.

2.1.5. Fungi:bacteria ratio

To quantify the presence of bacteria and fungi in the aggregates, we performed phospholipid fatty acid analysis (PLFA). Lipids were extracted using a modified Bligh and Dyer (1959) protocol (Frostegård and Bååth, 1996), subject to silica solid phase extraction using a method adapted from Mills and Goldhaber (2010), then the polar fraction (methanol eluate) was subject to mild alkaline hydrolysis and analysed by Gas Chromatography-Mass Spectrometry (GC–MS) (GCMS-QP2010Plus, Shimadzu, Kyoto, Japan).

The phospholipid fatty acid biomarkers were assigned to seven microbial categories: C14:0, C15:0 and C17:0 for general bacteria i-C15:0, a-C15:0, i-C16:0, i-C17:0, a-C17:0 for gram-positive bacteria 2-OH-C14:0, C16:1 w7c, C18:1w7c/C18:1w9t, C18:1w5c for gram-negative bacteria 10MeC18:0 for actinobacteria C16:1 w5c for mycorrhizal fungi C18:2 w6c for saprophytic fungi and C18:1w9c for fungi (Willers et al., 2015; Ullah et al., 2021; Kong et al., 2010).

Wet sieving may cause differential loss of microbial cells and could alter the microbial community composition estimates in the aggregates by PLFA (Felde et al., 2021). However, we reason that comparisons among treatments are valid because all treatments were subject to the same wet sieving protocol.

2.1.6. Metabolites

Water-extractable extracellular low molecular weight organic metabolites in aggregates (180 days of incubation) were extracted with ultrapure water (1 g soil: 10 mL water) by shaking for 2 h at 100 rpm using a reciprocating shaker. The metabolites were analysed using Gas Chromatography-Mass Spectrometry (GC–MS) (GCMS-QP2010Plus, Shimadzu, Kyoto, Japan). For GC–MS, 5 μL of 20 μg mL^{-1} ribitol (internal standard) was added to each dried sample, which was then re-dried for 1 h and derivatised with 40 μL methoxyamination reagent (20 mg mL^{-1} methoxyamine hydrochloride in pyridine) and 70 μL N-Methyl-N-trifluoroacetamide (MSTFA) (Warren, 2014; Rabbi et al., 2021).

2.1.7. Pore geometry

We scanned 3 oven-dried (at 40 °C) representative aggregates (500–2000 μm) per treatment using X-ray microtomography. The aggregates were packed in layers in 5 mm polypropylene tubes and separated by a piece of polystyrene foam to easily identify each aggregate in CT image volumes. All the samples were scanned using a GE X-ray tube (GE, Germany) fitted with a flatbed detector of high voxel and spatial resolution (3000 × 3000 pixels) and a helical scanning system. The samples were scanned with 360° rotation and 6-μm voxel resolution at 120 kV and 150 μA with a 2 mm Al filter placed in front of the detector. The pores in the aggregates were segmented using the histogram based manual thresholding in Fiji (Schindelin et al., 2012; Rabbi et al., 2015b). The pore size distribution was calculated using maximum inscribed sphere in pores (Hildebrand and Rüegsegger, 1997). The frequency distribution of 15–60 μm and > 60 μm pores in aggregates was estimated using BoneJ2 and the count of the pores were adjusted to 1 cm^2 area of the aggregates.

2.2. Statistical analysis

Two-way analysis of variance (ANOVA) was performed in R version 4.1.0 (R Core Team, 2018) to determine the influence of types of carbon and water treatments on the soil respiration, aggregate mass, metabolite concentrations, aggregate associated carbon, microbially derived carbon, fungi:bacteria ratio, and pore geometry (porosity, 15–60 μm and > 60 μm pores). The adequacy of the ANOVA models was assessed by checking normal Q-Q, residual vs fitted and Cook's distance plots. Response variables were transformed if the data was not normal. The *post-hoc* comparison between treatments was performed using the TukeyHSD in R when the interaction term in the ANOVA model was not significant. Constrained-redundancy analysis (RDA) was performed in Canoco 5.0 (Microcomputer Power, Ithaca, USA) to show the differences in metabolite concentrations in different carbon and water treatments (ter Braak and Smilauer, 2012).

3. Results

3.1. Soil respiration and aggregate mass

The rate of respiration of glucose and cellulose treated soils was 7 times higher than the control ($P < 0.0001$), and unaffected by water treatment after 180 days of incubation (Fig. 1a). There were similar differences in respiration between treatments at 30, 60, 90 days of incubation (Supplementary Materials). The wet-dry treatment had significantly higher (~2 times) aggregate mass on average across carbon types after 180 days of incubation compared to the wet treatment ($P < 0.01$) (Fig. 1b). The glucose treatment had 3 to 4 times more aggregate mass (500–2000 μm) than cellulose and control ($P < 0.0001$).

3.2. Carbon content, microbially derived carbon and fungi:bacteria ratio

The average content of carbon in aggregates of cellulose treated soil was 3 and 4 times higher ($P < 0.0001$) than that of glucose and control, respectively (Fig. 1c). The carbon content of aggregates did not differ between wet and wet-dry treatments. On average, 94 % (95 % confidence interval 87 % – 100 %) of carbon in the control was microbially derived carbon, whereas microbially derived carbon was 57 % (95 % confidence interval 44 % – 69 %) in glucose treatment and 17 % (95 % confidence interval 7 % – 27 %) in cellulose treatment ($P < 0.0001$) (Fig. 1d). The fraction of microbially derived carbon did not differ between wet and wet-dry treatments.

Raman micro-spectroscopic mapping of glucose treatment under wet and wet-dry water regimes demonstrated multiple small patches with spectra consistent with protein, lipid, amide, and phospholipid in aggregates, whereas in control there were no distinct patches of spectra associated with organic compounds (Fig. 2a).

The PLFA biomarkers-based fungi:bacteria ratio showed that fungi were the dominant microbes in aggregates. The ratio of fungal to bacterial biomarkers was 4 in glucose treated aggregates and 7 in cellulose treated aggregates (Fig. 2b) ($P < 0.01$). The fungi:bacteria ratio was not statistically different between wet and wet-dry treatments.

3.3. Metabolites

We identified 21 low molecular weight extracellular metabolites

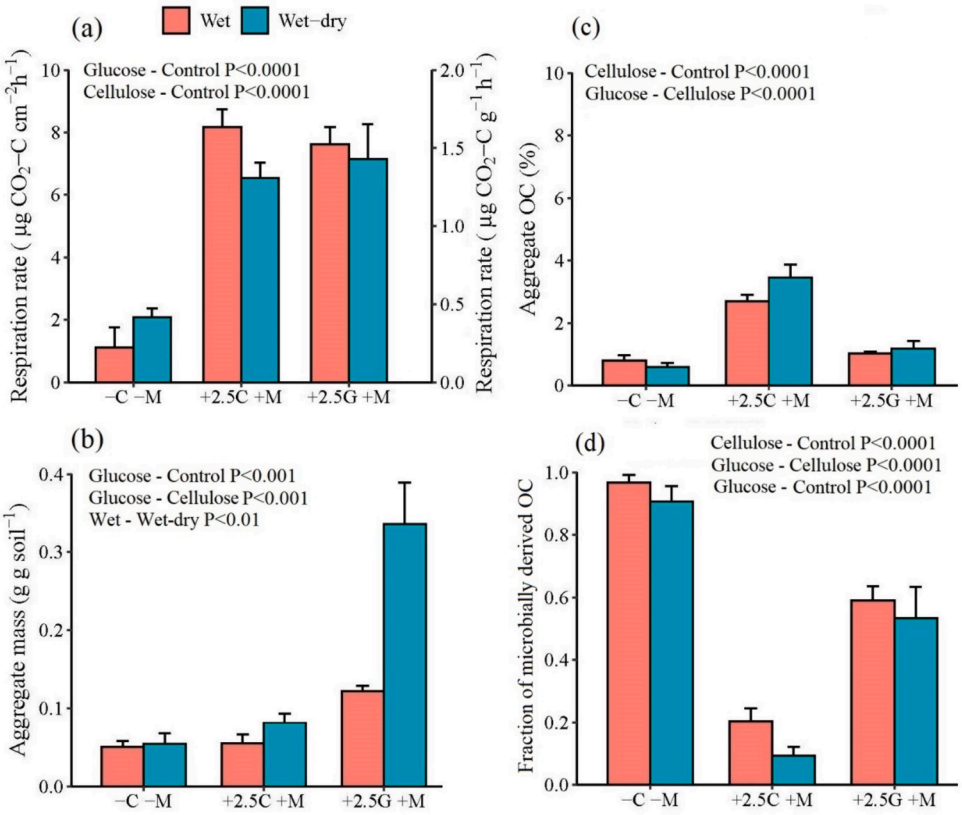

Fig. 1. Soil respiration rate (expressed in µg CO_2-C $cm^{-2}h^{-1}$ and µg CO_2-C $g^{-1}h^{-1}$) (a), aggregate mass (500–2000 µm) (g g $soil^{-1}$) (b), aggregate organic carbon (OC) (%) (c) and fraction of microbially derived OC (d) after 180 days of incubation with 2.5 % carbon in wet and wet-dry conditions. –C–M = no carbon + no microbe, +2.5G + M = 2.5 % carbon as glucose + microbe, +2.5C + M = 2.5 % carbon as cellulose + microbe. The vertical lines on the bars are the standard error of means (n = 4). Insets showing significant main effects and interaction between treatments in TukeyHSD *post-hoc* analysis.

such as sugars, sugar alcohols, organic acids, and nitrogen-containing compounds like pyroglutamic acid (Fig. 3a). The total carbon concentration of the extracted metabolites was on average 6 % of the total organic carbon content of aggregates. The concentration of glucose, trehalose, mannitol, galactonic acid and citric acid accounted for > 90 % of total metabolite concentration in all carbon and microbe treatments in wet and wet-dry water regimes (Fig. 3b). The RDA plot shows that the metabolite concentration in the aggregates of glucose treatments was significantly different than cellulose and control treatments ($P < 0.05$) (Fig. 3a). Glucose, trehalose, gentiobiose, fructose, citric acid, galactonic acid, mannitol, and galactitol concentrations in aggregates of the glucose treated soils was significantly higher than cellulose treated soils and control ($P < 0.0001$). There was no significant difference in metabolite concentration between wet and wet-dry treatments.

3.4. Pore geometry

The aggregates produced in wet-dry treatment had 2 times greater porosity compared to the wet treatment ($P < 0.05$), whereas the porosity in the aggregates of cellulose treated soils was not significantly different from the glucose and control treatment (Fig. 4a, b & Supplementary Materials). The number of > 60 µm pores did not differ among treatments (Fig. 4c). In the wet-dry treatment the number of pores between 15 and 60 µm was 3 times lower in glucose and cellulose treatment soils compared to the control, whereas pore count in the wet treatment was 2 times higher in control and cellulose than glucose treatment (i.e., water × carbon type rate interaction $P < 0.05$) (Fig. 4d).

4. Discussion

The microbial decomposition of organic matter produces different arrays of depolymerisation products in soil, such as sugars, amino acids, and compounds with methoxyl or carboxyl groups (Warren, 2016; Bucka et al., 2021). Our work extends the findings of Kallenbach et al. (2016) who showed that microbes receiving sugar and syringol were able to produce protein, lipid, and chitin in soils incubated under conditions like our experimental system. We show here that microbially mediated processes not only give rise to a diverse array of metabolites and organic macro-molecules, but also affect soil aggregation. Based on the findings of the current work we present a pictorial summary of the biophysical processes of aggregation in Fig. 5.

Multiple lines of evidence demonstrate microbes play a pivotal role in the aggregation of glucose treated soils. First, respiration rate was significantly higher in those soils with greater aggregation. Secondly, glucose derived aggregates were characterised by the presence of a range of proteins, lipids, amides, phospholipids, extracellular sugar alcohols and amino and organic acids that must have been products of microbial synthesis or synthesis followed by decomposition. The microbial origin of the diverse metabolites is supported by the presence of higher fungi:bacteria ratio and $\delta^{13}C$ evidence of a greater fraction of microbially derived carbon in the glucose treatment than the control.

Aggregation was associated with the presence of a diversity of extracellular metabolites of microbial origin, but it is unclear if metabolites are causally related to aggregation. We know that metabolites interact with mineral surfaces *via* cation linkages (Kleber et al., 2021) and the metabolite binding capacity depends on chemical structure (Naveed et al., 2017; Akhtar et al., 2018; Galloway et al., 2020; Kleber et al., 2021). Previous studies showed individual metabolites may either

(a)

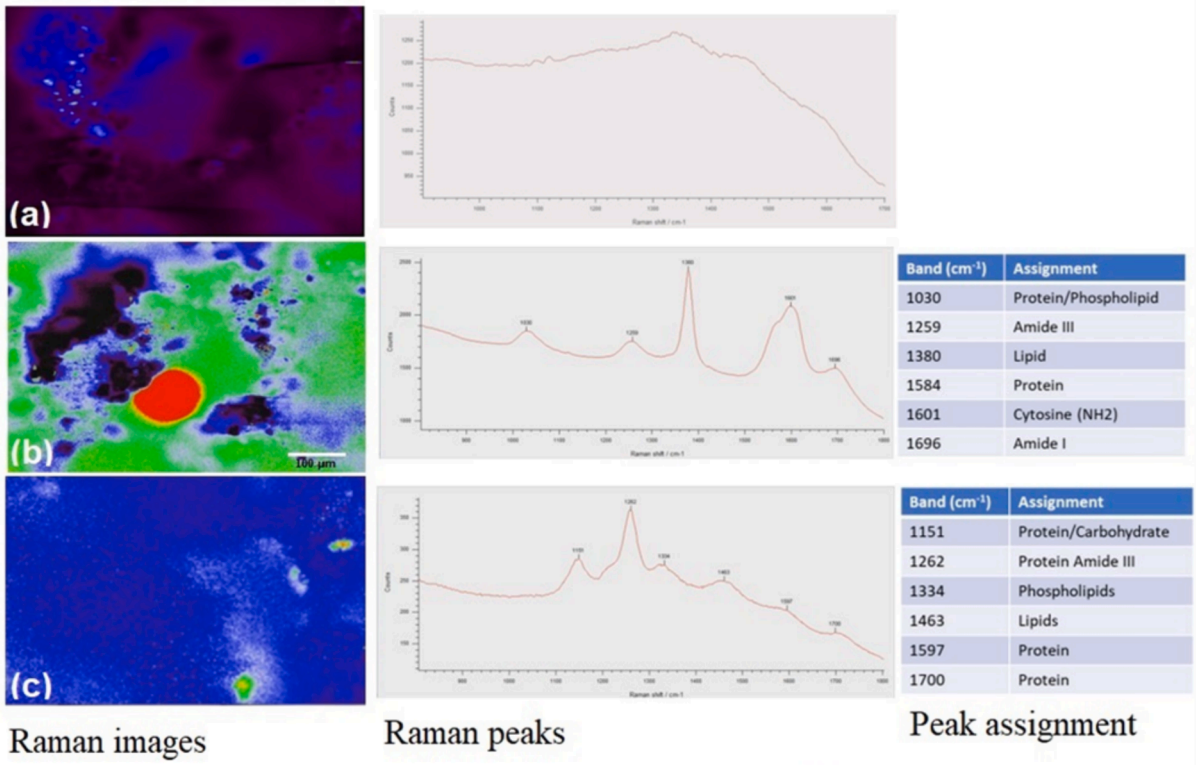

Band (cm^{-1})	Assignment
1030	Protein/Phospholipid
1259	Amide III
1380	Lipid
1584	Protein
1601	Cytosine (NH2)
1696	Amide I

Band (cm^{-1})	Assignment
1151	Protein/Carbohydrate
1262	Protein Amide III
1334	Phospholipids
1463	Lipids
1597	Protein
1700	Protein

(b)

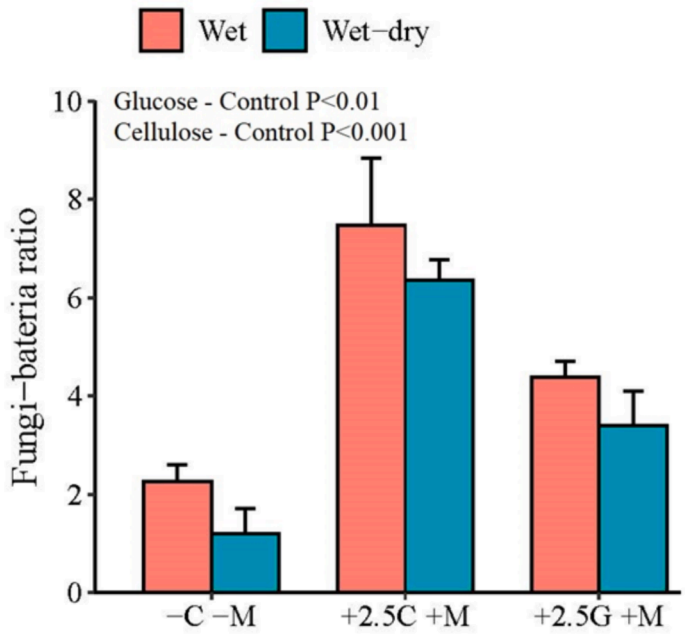

Fig. 2. Raman microscope images of microbial macro-molecule on the aggregate surface and associated peaks and peak assignment (a). The false colours in each Raman microscope image represent clusters of peaks produced by principal component analysis. Red and yellow zones indicate microbially derived macro-molecules, whereas green and blue zones indicate soil matrix. Raman peaks represent Raman shift (cm^{-1}) and peak intensity (counts). The Raman peak assignments are also shown. Fungi:bacteria ratio in soil aggregates after 180 days of incubation with 2.5 % carbon in wet and wet-dry conditions (b). –C–M = no carbon + no microbe, +2.5G + M = 2.5 % carbon as glucose + microbe, +2.5C + M = 2.5 % carbon as cellulose + microbe. The vertical lines on the bars are the standard error of means (n = 4). Insets showing significant main effects and interaction between treatments in TukeyHSD post-hoc analysis.

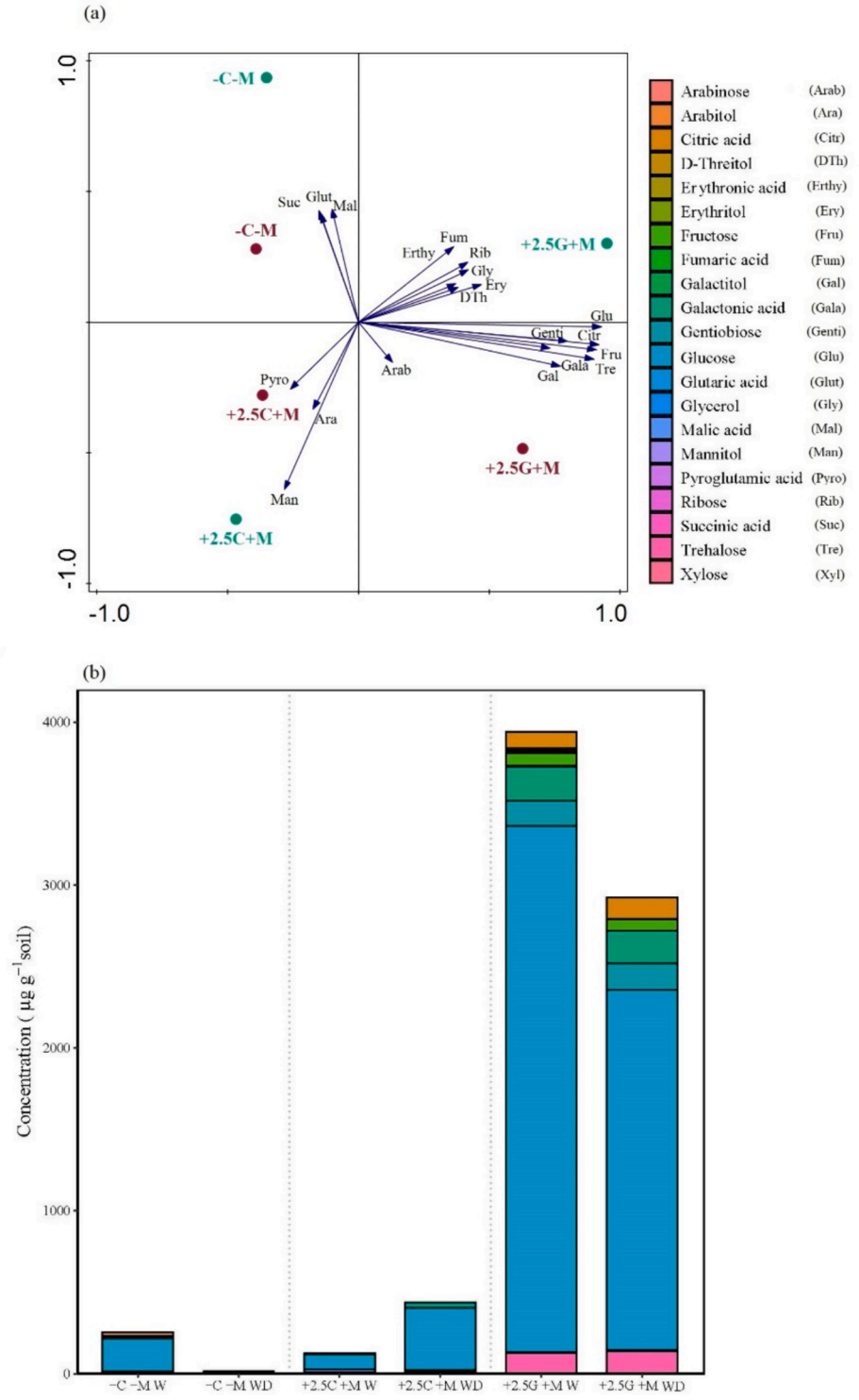

Fig. 3. Redundancy analysis biplot (a) showing the separation of metabolites and bar plot showing metabolite concentration in soil aggregates (µg g soil^{-1}) (b) after 180 days of incubation with 2.5 % carbon in wet and wet-dry conditions. In the biplot light green is wet and dark red is wet-dry treatment. –C–M = no carbon + no microbe, +2.5G + M = 2.5 % carbon as glucose + microbe, +2.5C + M = 2.5 % carbon as cellulose + microbe, W = wet, WD = wet-dry.

increase or decrease the stability of the aggregates (Naveed et al., 2017). For example, addition of maize root exudates comprising sugars, sugar alcohol, amino acids, organic acids, and fatty acids stabilised the soil (Naveed et al., 2017), whereas in other studies organic acids were reported to destabilise the soil (Keiluweit et al., 2015). The absence of consistent findings in studies applying exogenous metabolites may be because metabolites are related to aggregation indirectly. For example, metabolites are indicative of microbial metabolism and thus associations between aggregation and extracellular metabolites could arise indirectly if microbial activity (i.e., growth, extracellular polysaccharide production) during decomposition of organic matter is what drives aggregation.

In our study, comparison of cellulose with glucose treatment suggested that decomposability of organic matter affects aggregation. The slow decomposability of cellulose (Miltner and Zech, 1998) is supported by only about 17 % of carbon present in the aggregates produced in

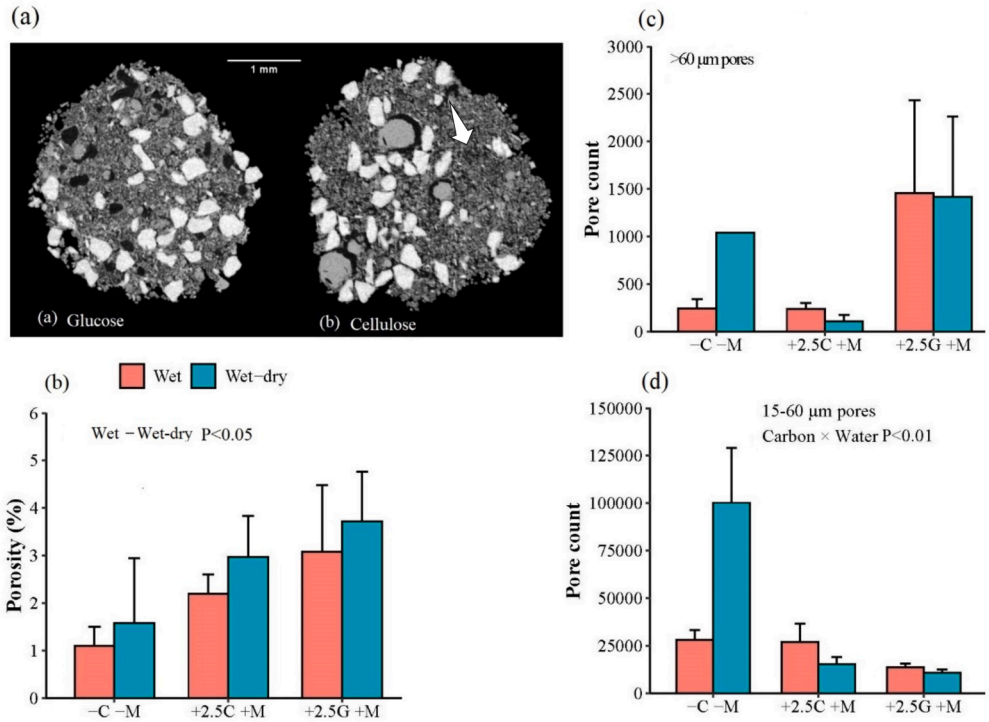

Fig. 4. Examples of 2D µCT slice of aggregates in glucose and cellulose treatments (a). On the 2D µCT slice white represent sand particles, dark grey is soil matrix and black within soil matrix is pores, µCT observed aggregate porosity (%) (b), count of >60 µm (c) and 15–60 µm pores (d) after 180 days of incubation with 2.5 % carbon in wet and wet-dry conditions. –C–M = no carbon + no microbe, +2.5G + M = 2.5 % carbon as glucose + microbe, +2.5C + M = 2.5 % carbon as cellulose + microbe. Arrow on (a) indicates cellulose fibre. It is important to note here, on µCT grayscale images both cellulose fibre and the fine soil matrix have similar grey value. The presence of cellulose fibre in the soil matrix can only be identified by close examination, as shown in Supplementary Materials. The vertical lines on the bars are the standard error of means (n = 4). Insets showing significant main effects and interaction between treatments in TukeyHSD *post-hoc* analysis.

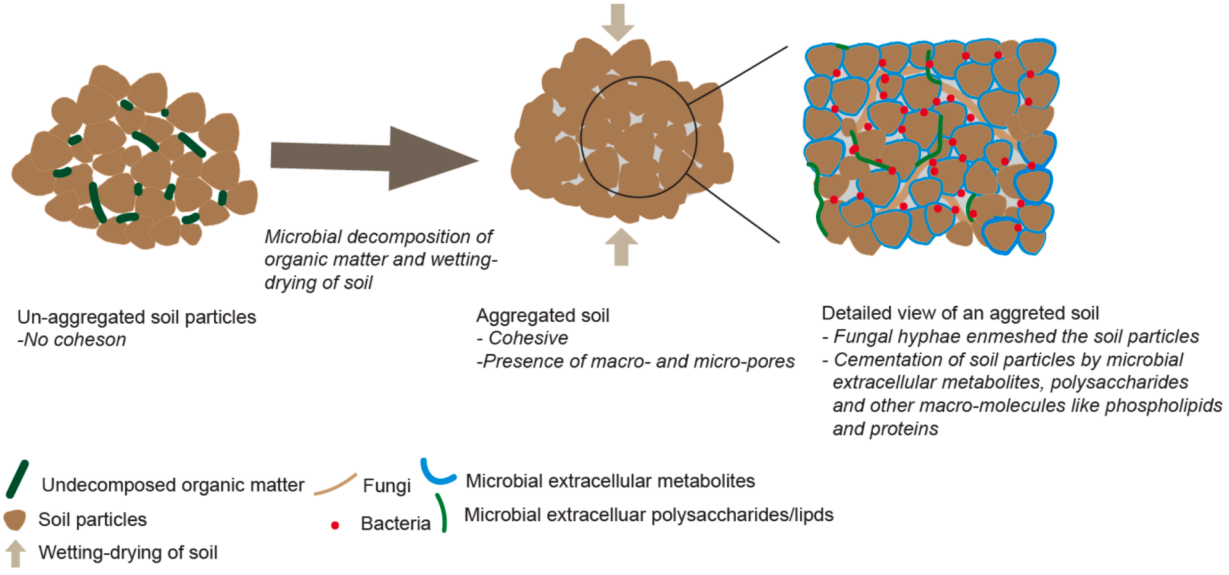

Fig. 5. Biophysical mechanisms of aggregation in soil.

cellulose treated soil being microbially derived versus 57 % in glucose treated soil. The presence of undecomposed cellulose (visible during wet-sieving and in 2D µCT image slices) (Fig. 4a and Supplementary Materials), high organic carbon content and low concentration of metabolites in cellulose-treated aggregates (especially in wet treatment) reinforced the low decomposability of the added cellulose. The lesser aggregation in the cellulose treatment, despite higher fungi:bacteria ratio, suggests a strong influence of microbial decomposition products in soil aggregation. The enmeshment of soil particles by fungal hyphae (Tisdall et al., 2012), hydrophobins, mycorrhizal glomalin (Rillig and Mummey, 2006) were thought to be the important factors of soil aggregation. However, recently Lehmann et al. (2020) showed that fungal morphology did not have strong relationship with the aggregate formation, which explain the less aggregation in the cellulose treatment with low concentration of microbial extracellular metabolites. Taken together these observations indicate decomposability of organic matter

is a dominant factor promoting aggregation (Rabbi et al., 2014; Sarker et al., 2018; Rabbi et al., 2020).

We observed about three times more aggregate mass under wet-dry compared to wet conditions in glucose-treated soil, supporting a role of wet-dry cycles in soil aggregation (Fig. 1b). Our data are consistent with reports that organic carbon decomposition and diffusion of dissolved organic carbon in the soil matrix can enhance aggregation during wet-dry cycles (Park et al., 2007; Possinger et al., 2020; Patel et al., 2021). The shrinkage and swelling of the soil matrix under wet-dry condition also alters the structure of the soil (Or, 1996; Diel et al., 2019; Xu et al., 2021). Although we did not observe crack formation under wet-dry conditions as observed in natural soils (Preston et al., 1999; Diel et al., 2019), the aggregate formation under wet-dry conditions was joint influence of the stabilisation of soil particles by microbially processed organic matter and development of cohesive strength during wet-dry cycles (Utomo and Dexter, 1982).

Aggregation was also observed, but to a much lesser extent (i.e., 3 times less than glucose treated soil) in the microbially suppressed controls that were not inoculated with microbes and did not receive glucose or cellulose (Fig. 1b). The uninoculated control had low concentrations and small number of extracellular metabolites and greatly reduced rates of respiration, indicating successful suppression of microbial growth and mechanistically explaining the reduced amount of aggregation. Other work suggests that the majority of aggregation in our uninoculated soils was probably produced by the physical or abiotic binding forces (i.e., phyllosilicate clays, wetting and drying) (Turk et al., 2011; Lavelle et al., 2020). For example, Denef and Six (2005) showed that kaolinitic soil can form aggregates even with limited organic matter input through physical and electrostatic interactions between clay minerals and polyvalent cations. Nevertheless, the evidence provided here highlights the dominant influence on soil aggregation was added organic matter and microbes rather than abiotic or mineralogical factors.

The increase in porosity of the aggregates was only observed between wet and wet-dry treatment (Fig. 4b). This contrast with evidence organic matter decomposition increases aggregate porosity (Feeney et al., 2006). Previous studies demonstrated that microbial activities create heterogeneous pores (Young et al., 2001; Crawford et al., 2012; Helliwell et al., 2014; Rabbi et al., 2015b; Harvey et al., 2020; Neal et al., 2020). Feeney et al. (2006) reported that the microbial decomposition of the organic matter and physical forces in the aggregates can promote the formation of pores. Feeney et al. (2006) also demonstrated that microbial activity significantly altered the soil micro-habitat toward a more porous and clustered structure. De Gryze et al. (2006) showed that the decomposition of organic matter could increase the proportion of 27–67 μm pores in the soil. However, the results we presented here did not corroborate the proposition that microbial activity due to addition of organic matter alters the porosity of aggregates (Feeney et al., 2006). The pore geometry changes that were reported in Feeney et al. (2006) and Gryze et al. (2006), unlike our experiment, used crop residues and naturally formed soils. Partial or complete microbial decomposition of the added organic matter in those previous studies probably influenced the formation of pores in aggregates. The clay minerals in natural soils are mixture of an array of phyllosilicates and oxides of iron and manganese. The physicochemical characteristics of these clay minerals and the interaction with microbes regulate the microbial functions (Kleber et al., 2021). However, the mixture of pure clay minerals is unable to mimic entirely the complexity of these processes. Crop residues contain polysaccharides, amino acids, and other macromolecules (Trinsoutrot et al., 2000), which was absent in pure glucose and cellulose. Therefore, it is expected that results of the current work will not be equivalent to the decomposition of organic matter in natural ecosystem but offers simplified way of understanding the natural processes. Nonetheless, the lower count of 15–60 μm pores in glucose and cellulose treated soils at wet-dry conditions compared to the control in the current experiment might suggest the development of cohesive strength in the newly formed aggregates and modification of pore geometry. Wetting-drying of soil also have contrasting effect on the aggregate stability. The stress generated by the wetting–drying at different water potentials increases aggregation, but it can also destabilise the aggregates during rapid wetting and drying cycles (Utomo and Dexter, 1982; Xu et al., 2021). Thus, the changes in aggregate porosity and pore size distribution in the current experiment was linked to the physical changes in the aggregates during wet-dry cycles (Fig. 4). Nonetheless, the altered porosity and pore size distribution in the aggregates regardless of its origin (microbial vs abiotic) has implications for fluid movement and carbon stabilisation in soil (Jastrow and Miller, 1998; Zhang et al., 2016).

5. Conclusion

Using artificial soil with known mineralogy and organic matter content, the current work demonstrated that wet-dry cycles and microbial decomposition of organic matter and subsequent synthesis of metabolites and macromolecules promote aggregation. The modification of pore geometry was driven mainly by the wet-dry cycles. The interconnected processes between extracellular metabolites, microbes and pore geometry we presented here suggested that the joint role of microbially derived carbon and abiotic process in stabilising the aggregates may vary with soil mineralogy, complexity of organic matter and microbial diversity, which requires further experimentation. Future research should focus on ways to better understand pore-scale biophysical processes in aggregates underpinning stabilisation of organic carbon and microbial function.

Credit authorship contribution statement

Sheikh M.F. Rabbi: Conceptualization, Experimentation, Methodology, Software, Data and Image analysis, Writing. **Charles R. Warren:** Conceptualization, Resources, Funding acquisition, Methodology, Software, Writing – review & editing. **Brad Swarbrick:** Methodology, Software, Visualization. **Budiman Minasny:** Conceptualization, Writing – review & editing. **Alex B. McBratney:** Conceptualization, Writing – review & editing. **Iain M. Young:** Conceptualization, Writing – review & editing.

Declaration of competing interest

The authors declare that they have no known competing financial interests or personal relationships that could have appeared to influence the work reported in this paper.

Data availability

Data will be made available on request.

Acknowledgments

We would like to thank Mr Ralph Faux, Technical Officer, The University of Sydney for his technical assistance for this work. This work was partially supported by a Discovery Grant (DP220101620) from the Australian Research Council.

Appendix A. Supplementary data

Supplementary data to this article can be found online at https://doi.org/10.1016/j.geoderma.2024.116924.

References

Abiven, S., Menasser, S., Chenu, C., 2009. The effects of organic inputs over time on soil aggregate stability-A literature analysis. SoilBiol. Biochem. 41, 1–12.

Akhtar, J., Galloway, A.F., Nikolopoulos, G., Field, K.J., Knox, P., 2018. A quantitative method for the high throughput screening for the soil adhesion properties of plant and microbial polysaccharides and exudates. Plant and Soil 428, 57–65.
Anderson, J.P.E., Domsch, K.H., 1978. A physiological method for the quantitative measurement of microbial biomass in soils. Soil Biol. Biochem. 10, 215–221.
Bergholt, M., Serio, A., Albro, M., 2019. Raman Spectroscopy: Guiding Light for the Extracellular Matrix. Front. Bioeng. Biotechnol. 7.
Bligh, E.G., Dyer, W.J., 1959. A rapid method of total lipid extraction and purification. Can. J. Biochem. Physiol. 37, 911–917.
Bucka, F.B., Felde, V.J.M.N.L., Peth, S., Kögel-Knabner, I., 2021. Disentangling the effects of OM quality and soil texture on microbially mediated structure formation in artificial model soils. Geoderma 403, 115213.
Crawford, J.W., Deacon, L., Grinev, D., Harris, J.A., Ritz, K., Singh, B.K., Young, I., 2012. Microbial diversity affects self-organization of the soil–microbe system with consequences for function. J. Royal Soc. Interface 9, 1302–1310.
De Gryze, S., Jassogne, L., Six, J., Bossuyt, H., Wevers, M., Merckx, R., 2006. Pore structure changes during decomposition of fresh residue: X-ray tomography analyses. Geoderma 134, 82–96.
Dechorgnat, J., Francis, K.L., Dhugga, K.S., Rafalski, J.A., Tyerman, S.D., Kaiser, B.N., 2018. Root Ideotype Influences Nitrogen Transport and Assimilation in Maize. Front. Plant Sci. 9.
Denef, K., Six, J., 2005. Clay mineralogy determines the importance of biological versus abiotic processes for macroaggregate formation and stabilization. Eur. J. Soil Sci. 56, 469–479.
Diel, J., Vogel, H.-J., Schlüter, S., 2019. Impact of wetting and drying cycles on soil structure dynamics. Geoderma 345, 63–71.
Feeney, D.S., Crawford, J.W., Daniell, T., Hallett, P.D., Nunan, N., Ritz, K., Rivers, M., Young, I.M., 2006. Three-dimensional microorganization of the soil-root-microbe system. Microbial Ecol. 52, 151–158.
Felde, V.J.M.N.L., Schweizer, S.A., Biesgen, D., Ulbrich, A., Uteau, D., Knief, C., Graf-Rosenfellner, M., Kögel-Knabner, I., Peth, S., 2021. Wet sieving versus dry crushing: Soil microaggregates reveal different physical structure, bacterial diversity and organic matter composition in a clay gradient. Eur. J. Soil Sci. 72 (2), 810–828.
Frostegård, A., Bååth, E., 1996. The use of phospholipid fatty acid analysis to estimate bacterial and fungal biomass in soil. Biol. Fertility. Soils 22, 59–65.
Galloway, A.F., Knox, P., Krause, K., 2020. Sticky mucilages and exudates of plants: putative microenvironmental design elements with biotechnological value. New Phytol. 225, 1461–1469.
Golchin, A., Oades, J.M., Skjemstad, J.O., Clarke, P., 1994. Soil structure and carbon cycling. Aus. J. Soil Res. 32, 1043–1068.
Harvey, H.J., Wildman, R.D., Mooney, S.J., Avery, S.V., 2020. Soil aggregates by design: Manufactured aggregates with defined microbial composition for interrogating microbial activities in soil microhabitats. Soil Biol. Biochem. 148, 107870.
Helliwell, J.R., Miller, A.J., Whalley, W.R., Mooney, S.J., Sturrock, C.J., 2014. Quantifying the impact of microbes on soil structural development and behaviour in wet soils. Soil Biol. Biochem. 74, 138–147.
Hildebrand, T., Rüegsegger, P., 1997. A new method for the model-independent assessment of thickness in three-dimensional images. J. Microscopy 185, 67–75.
Jastrow, J.D., Miller, R.M., 1998. Soil aggregate stabilization and carbon sequestration: Feedbacks through organomineral associations. In: Lal, R., Kimble, J.M., Follett, R. F., Stewart, B.A. (Eds.), Soil Processess and the Carbon Cycle. CRC Press, Boca raton, pp. 207–223.
Kallenbach, C.M., Frey, S.D., Grandy, A.S., 2016. Direct evidence for microbial-derived soil organic matter formation and its ecophysiological controls. Nat. Commun. 7, 13630.
Keiluweit, M., Bougoure, J.J., Nico, P.S., Pett-Ridge, J., Weber, P.K., Kleber, M., 2015. Mineral protection of soil carbon counteracted by root exudates. Nat. Clim. Chang. 5, 588–595.
Kleber, M., Bourg, I.C., Coward, E.K., Hansel, C.M., Myneni, S.C.B., Nunan, N., 2021. Dynamic interactions at the mineral–organic matter interface. Nat. Rev. Earth Environ. 2, 402–421.
Kong, A.Y.Y., Scow, K.M., Cordova-Kreylos, A.L., Holmes, W.E., Six, J., 2010. Microbial community composition and carbon cycling within soil microenvironments of conventional, low-input, and organic cropping systems. Soil Biol. Biochem. 43, 20–30.
Lavelle, P., Spain, A., Fonte, S., Bedano, J.C., Blanchart, E., Galindo, V., Grimaldi, M., Jimenez, J.J., Velasquez, E., Zangerlé, A., 2020. Soil aggregation, ecosystem engineers and the C cycle. Acta Oecol. 105, 103561.
Lehmann, A., Zheng, W., Ryo, M., Soutschek, K., Roy, J., Rongstock, R., Maaß, S., Rillig, M.C., 2020. Fungal traits important for soil aggregation. Front. Microbiol. 10.
Mills, C.T., Goldhaber, M.B., 2010. On silica-based solid phase extraction techniques for isolating microbial membrane phospholipids: Ensuring quantitative recovery of phosphatidylcholine-derived fatty acids. Soil Biol. Biochem. 42, 1179–1182.
Miltner, A., Zech, W., 1998. Carbohydrate decomposition in beech litter as influenced by aluminium, iron and manganese oxides. Soil Biol. Biochem. 30, 1–7.
Moebius-Clune, B.N., Moebius-Clune, D.J., Gugino, B.K., Idowu, O.J., Schindelbeck, R.R., Ristow, A.J., Es, H.M.V., Thies, J.E., Shayler, H.A., McBride, M.B., Wolfe, D.W., Abawi, G.S., 2016. Comprehensive Assessment of Soil Health – The Cornell Framework Manual, Edition 3.0. Cornell University, Geneva, NY.
Movasaghi, Z., Rehman, S., Rehman, I.U., 2007. Raman spectroscopy of biological tissues. Appl. Spectrosc. Rev. 42, 493–541.
Naveed, M., Brown, L.K., Raffan, A.C., George, T.S., Bengough, A.G., Roose, T., Sinclair, I., Koebernick, N., Cooper, L., Hackett, C.A., Hallett, P.D., 2017. Plant exudates may stabilize or weaken soil depending on species, origin and time. Eur. J. Soil Sci. 68, 806–816.
Neal, A.L., Bacq-Labreuil, A., Zhang, X., Clark, I.M., Coleman, K., Mooney, S.J., Ritz, K., Crawford, J.W., 2020. Soil as an extended composite phenotype of the microbial metagenome. Sci. Rep. 10, 10649.
Nunan, N., Leloup, J., Ruamps, L.S., Pouteau, V., Chenu, C., 2017. Effects of habitat constraints on soil microbial community function. Sci. Rep. 7.
Oades, J.M., 1993. The role of biology in the formation, stabilization and degradation of soil structure. Geoderma 56, 377–400.
Or, D., 1996. Wetting-induced soil structural changes: The theory of liquid phase sintering. Water Resour. Res. 32 (10), 3041–3049.
Park, E.J., Sul, W.J., Smucker, A.J.M., 2007. Glucose additions to aggregates subjected to drying/wetting cycles promote carbon sequestration and aggregate stability. Soil Biol. Biochem. 39, 2758–2768.
Patel, K.F., Myers-Pigg, A., Bond-Lamberty, B., Fansler, S.J., Norris, C.G., McKever, S.A., Zheng, J., Rod, K.A., Bailey, V.L., 2021. Soil carbon dynamics during drying vs. rewetting: Importance of antecedent moisture conditions. Soil Biol. Biochem. 156.
Pausch, J., Kuzyakov, Y., 2012. Soil organic carbon decomposition from recently added and older sources estimated by δ13C values of CO2 and organic matter. Soil Biol. Biochem. 55, 40–47.
Phillips, D.L., Gregg, J.W., 2001. Uncertainty in source partitioning using stable isotopes. Oecologia 127 (2), 171–179.
Possinger, A.R., Bailey, S.W., Inagaki, T.M., Kögel-Knabner, I., Dynes, J.J., Arthur, Z.A., Lehmann, J., 2020. Organo-mineral interactions and soil carbon mineralizability with variable saturation cycle frequency. Geoderma 375, 114483.
Preston, S., Griffiths, B.S., Young, I.M., 1999. Links between substrate additions, native microbes, and the structural complexity and stability of soils. Soil Biol. Biochem. 31, 1541–1547.
R Core Team, 2018. R: A language and environment for statistical computing. R Foundation for Statistical Computing, Vienna, Austria http://www.R-project.org/.
Rabbi, S.M.F., Linser, R., Hook, J.M., Wilson, B.R., Lockwood, P.V., Daniel, H., Young, I. M., 2014. Characterization of soil organic matter in aggregates and size-density fractions by solid state 13C CPMAS NMR spectroscopy. Commun. Soil Sci. Plant Anal. 45, 1523–1537.
Rabbi, S.M.F., Tighe, M., Delgado-Baquerizo, M., Cowie, A., Robertson, F., Dalal, R., Page, K., Crawford, D., Wilson, B.R., Schwenke, G., McLeod, M., Badgery, W., Dang, Y.P., Bell, M., O'Leary, G., Liu, D.L., Baldock, J., 2015. Climate and soil properties limit the positive effects of land use reversion on carbon storage in Eastern Australia. Sci. Rep. 5, 17866.
Rabbi, S.M.F., Wilson, B.R., Lockwood, P.V., Daniel, H., Young, I.M., 2015b. Aggregate hierarchy and carbon mineralization in two Oxisols of New South Wales, Australia. Soil Tillage Res. 146 (Part B), 193–203.
Rabbi, S.M.F., Minasny, B., McBratney, A.B., Young, I.M., 2020. Microbial processing of organic matter drives stability and pore geometry of soil aggregates. Geoderma 360.
Rabbi, S.M.F., Tighe, M.K., Warren, C.R., Zhou, Y., Denton, M.D., Barbour, M.M., Young, I.M., 2021. High water availability in drought tolerant crops is driven by root engineering of the soil micro-habitat. Geoderma 383, 114738.
Rillig, M.C., Mummey, D.L., 2006. Mycorrhizas and soil structure. New Phytol. 171, 41–53.
Sarker, T.C., Incerti, G., Spaccini, R., Piccolo, A., Mazzoleni, S., Bonanomi, G., 2018. Linking organic matter chemistry with soil aggregate stability: Insight from 13C NMR spectroscopy. Soil Biol. Biochem. 117, 175–184.
Schindelin, J., Arganda-Carreras, I., Frise, E., Kaynig, V., Longair, M., Pietzsch, T., Preibisch, S., Rueden, C., Saalfeld, S., Schmid, B., Tinevez, J.-Y., White, D.J., Hartenstein, V., Eliceiri, K., Tomancak, P., Cardona, A., 2012. Fiji: an open-source platform for biological-image analysis. Nat. Methods 9, 676–682.
Southard, R.J., Buol, S.W., 1988. Subsoil Blocky Structure Formation in Some North Carolina Paleudults and Paleaquults. Soil Sci. Soc. Am. J. 52, 1069–1076.
Ter Braak, C.J.F., Smilauer, P., 2012. Canoco reference manual and users' guide:software for ordination (version 5.0). Microcomputer Power, Ithaca, New York.
Tisdall, J.M., Nelson, S.E., Wilkinson, K.G., Smith, S.E., McKenzie, B.M., 2012. Stabilisation of soil against wind erosion by six saprotrophic fungi. Soil. Biol. Biochem. 50, 134–141.
Tisdall, J.M., Oades, J.M., 1982. Organic matter and water stable aggregates in soils. J. Soil Sci. 33, 141–163.
Trinsoutrot, I., Recous, S., Bentz, B., Lineres, M., Cheneby, D., Nicolardot, B., 2000. Biochemical quality of crop residues and carbon and nitrogen mineralization kinetics under nonlimiting nitrogen conditions. Soil Sci. Soc. Am. J. 64 (3), 918–926.
Turk, J.K., Chadwick, O.A., Graham, R.C., 2011. Pedogenic processes. In: Huang, P.M., Li, Y., Sumner, M.E. (Eds.), Handbook of Soil Sciences: Properties and Processes, second ed. Taylor & Francis Group, Baton Rouge, USA.
Ullah, M.R., Carrillo, Y., Dijkstra, F.A., 2021. Drought-induced and seasonal variation in carbon use efficiency is associated with fungi:bacteria ratio and enzyme production in a grassland ecosystem. Soil Biol. Biochem. 155.
Utomo, W.H., Dexter, A.R., 1982. Changes in soil aggregate water stability induced by wetting and drying cycles in non-saturated soil. Eur. J. Soil Sci. 33, 623–637.
Warren, C.R., 2014. Response of osmolytes in soil to drying and rewetting. Soil Biol. Biochem. 70, 22–32.
Warren, C.R., 2016. Do microbial osmolytes or extracellular depolymerisation products accumulate as soil dries? Soil Biol. Biochem. 98, 54–63.
Willers, C., Jansen van Rensburg, P.J., Claassens, S., 2015. Phospholipid fatty acid profiling of microbial communities-a review of interpretations and recent applications. J. Appl. Microbiol. 119, 1207–1218.
Witzgall, K., Vidal, A., Schubert, D.I., Höschen, C., Schweizer, S.A., Buegger, F., Pouteau, V., Chenu, C., Mueller, C.W., 2021. Particulate organic matter as a functional soil component for persistent soil organic carbon. Nat. Commun. 12, 4115.

WRB, 2015. International soil classification system for naming soils and creating legends for soil maps. World Reference Base for Soil Resources (WRB). IUSS Working Group, World Soil Resources Reports No. 106. FAO, Rome.
Xu, X.-T., Shao, L.-J., Huang, J.-B., Xu, X., Liu, D.-Q., Xian, Z.-X., Jian, W.-B., 2021. Effect of wet-dry cycles on shear strength of residual soil. Soil. Found. 61, 782–797.
Young, I.M., Crawford, J.W., Rappoldt, C., 2001. New methods and models for characterising structural heterogeneity of soil. Soil Tillage Res. 61, 33–45.
Zhang, X., Crawford, J.W., Flavel, R.J., Young, I.M., 2016. A multi-scale Lattice Boltzmann model for simulating solute transport in 3D X-ray micro-tomography images of aggregated porous materials. J. Hydrol. 541 (Part B), 1020–1029.